Dynamic correlations of the classical and quantum Toda lattice

A. Cuccoli, M. Spicci, and V. Tognetti
Dipartimento di Fisica dell'Università di Firenze, Largo E. Fermi 2, I-50125 Firenze, Italy

R. Vaia
Istituto di Elettronica Quantistica del Consiglio Nazionale delle Ricerche, Via Panciatichi 56/30, I-50127 Firenze, Italy
(Received 22 September 1992)

The dynamic correlations of classical and quantum Toda lattices are approached by moment expansion. For the classical model, the moments of the spectral shape of the displacement-displacement correlation function are exactly calculated up to the eighth one, while, for the quantum system, their evaluation is limited to the sixth one, using the effective-potential method in low-coupling approximation. The spectral shape is calculated using the continued-fraction expansion. The relevance of quantum effects is clearly shown, in dependence on temperature and quantum coupling. At all wave vectors, the spectral shape presents a single-peak structure, both in the classical and in the quantum regime.

I. INTRODUCTION

In the last two decades a large amount of work has been devoted to the study of the dynamic and statistical properties of nonlinear systems.[1] One of the motivations of such interest is surely the realization that the combination of variety, beauty, and stability observed in the most complex structures existing in nature, biological systems included, is largely due to their intrinsic nonlinear character. However, a comprehensive machinery, like that one developed for the linear systems, able to allow a unified treatment of any nonlinear structure, has not yet been developed. Due to the difficulty of the general problem, many efforts have therefore been devoted to the identification and investigation of the simplest nonlinear models, for which rigorous results can be drawn and exact solutions in particular cases can be found. Also these elementary systems, however, despite their apparent simplicity, give rise to a variety of behavior, and provide a formidable challenge both from the physical and from the mathematical point of view.

Among such models we consider the one-dimensional lattice with nearest-neighbor exponential interaction, introduced by Toda in the late sixties.[2–4] The main feature of this model is its integrability, so that exact solutions of the equations of motion for the lattice can, in principle, be found for given initial conditions. Moreover, particular solutions, having a solitonic character, can be found for the same equation. Also the classical partition function of the Toda chain can be calculated in closed form, so that the macroscopic, equilibrium thermodynamic functions can be exactly evaluated.[5]

However, the capability of solving the equations of motion and producing the exact partition function does not imply, by any means, that the more interesting problem of evaluating the nonequilibrium statistical properties of the system can be equally easily addressed. The relevance of the last problem is apparent by recalling that the most detailed information about the behavior and the role played by the elementary excitations of a system is not contained in the static quantities but in the dynamic correlation function. It is just the last one that determines, for example, the response function in neutron-scattering experiments, and strictly related to it are other characteristic quantities, probed by other spectroscopies, such as, for example, the relaxation times.

The dynamic correlation functions of nonlinear integrable systems can be exactly evaluated only in few simple cases.[6] Up to today, the Toda lattice is not inserted in this list. Numerical simulations, based on molecular dynamics (MD), can be used for classical systems. However, difficulties occur in approaching the thermodynamic equilibrium, due to the presence of an infinity of conserved quantities as a consequence of integrability. Therefore, the pioneering simulations did not give definite results[7] and were repeated only recently.[8] We are not aware of any attempt to study the dynamic correlation function of the quantum Toda lattice. For the classical model, the most detailed investigation was made by Diederich,[9–11] who derived and solved a set of nonlinear integrodifferential equations for the correlation functions in the reciprocal space. This approach is essentially a mode-coupling theory, similar to that developed by Blume and Hubbard to address the same problem in Heisenberg ferromagnets,[12] and by Kawasaki to study a lot of physical systems in a neighborhood of the critical point.[13] The most striking result obtained by Diederich is the appearance in the spectral shape, for intermediate wave vectors, of a second peak, which Diederich attributes to solitonic excitations. However, such features in the spectra are not confirmed by other calculations.[7] Although the dynamic correlation calculated within the diluted soliton-gas approximation[14]— whose application could perhaps be questionable, the Toda solitons being

gapless — results from two independent contributions at each wave vector, one coming from phonons and the other one from solitons, centered at two slightly different frequencies, the soliton peak is almost completely absorbed in the wing of the phonon component once the intensities of the two peaks are correctly taken into account. Moreover, we have repeated the mode-coupling calculations, and they did not reproduce the two-peaked structures, in agreement with new recent MD simulations.[8] As shown in this paper, the absence of the soliton peak is also confirmed by our moment analysis.

In this paper the dynamic line shape of the Toda lattice is addressed from a different point of view, valid both in the classical and quantum case. We give some definite information about the properties of the dynamic response function through the evaluation of its frequency moments. Such quantities can indeed be expressed as static correlation functions, so that they can be exactly evaluated in the classical system and approximately also in the quantum one.[15] Explicit results for the lowest-order moments (up to the eighth classical one and the sixth quantum one) are given as functions of temperature, and a reconstruction of the line shape starting from the knowledge of the first coefficients of its continued fraction expansion is presented. This analysis allows us to have information on quantum dynamic correlations, and we show that our set of moments seems to be inconsistent with a double-peaked structure both for classical and quantum systems.

II. THE CORRELATION FUNCTIONS OF THE TODA LATTICE

The Toda lattice is a one-dimensional array of N particles of mass m, interacting through an exponential nearest-neighbor interaction potential $v(r)$. Its Hamiltonian reads

$$\hat{\mathcal{H}} = \sum_{i=1}^{N} \left[\frac{\hat{p}_i^2}{2m} + v(\hat{x}_i - \hat{x}_{i-1}) \right] , \tag{2.1}$$

$$v(r) = \frac{a}{b} \left[e^{-b(r-r_0)} - 1 \right] + a(r - r_0) . \tag{2.2}$$

The constant b^{-1} fixes the length scale over which the nonlinearity of the potential shows up, while the ratio a/b sets the energy scale. The value of $r = r_0$, corresponding to the minimum of $v(r)$, represents also the equilibrium distance of two adjacent particles at zero temperature and zero pressure in the classical system. The relevance of quantum effects is measured through the dimensionless coupling constant:

$$g \equiv (\hbar\omega_0)/(a/b) = (\hbar b^{\frac{3}{2}})/\sqrt{am} , \tag{2.3}$$

$$\omega_0 = \sqrt{v''(r_0)/m} = \sqrt{ab/m} , \tag{2.4}$$

i.e., the ratio between the characteristic energy $\hbar\omega_0$ of the quantum harmonic excitations and the overall energy scale a/b of the system. All the results given in the following are obtained for periodic boundary conditions and in the thermodynamic limit ($N \to \infty$ and $L \to \infty$ with $d = L/N$ held constant, L being the total length of the chain).

To investigate the dynamic behavior of the system, we will consider the correlation function:

$$C(k,\omega) = -\frac{1}{N} \sum_{ij} e^{-ikd(i-j)} \int dt e^{i\omega t} \left\langle [\hat{u}_i(t) - \hat{u}_j(0)]^2 \right\rangle , \tag{2.5}$$

where $\hat{u}_i(t) \equiv \hat{x}_i(t) - id$ is the "displacement" of the ith atom at time t from its equilibrium position. In the thermodynamic limit, $C(k,\omega)$ is well defined for every value of the frequency ω and for all wave vectors k of the first Brillouin zone $[-\frac{\pi}{a}, \frac{\pi}{a}]$. For $k \neq 0$, $C(k,\omega)$ is proportional to the symmetrized correlation function, which determines the response of the system in a neutron-scattering experiment:

$$C(k,\omega) = 2 \left[\frac{1}{N} \sum_{ij} e^{-ikd(i-j)} \int dt e^{i\omega t} \frac{1}{2} \langle \hat{u}_i(t)\hat{u}_j(0) + \hat{u}_j(0)\hat{u}_i(t) \rangle \right] . \tag{2.6}$$

$C(k,\omega)$ can be easily related also to other dynamic response functions of the Toda lattice considered in the literature;[7,9–11] for example, in the classical case and for $k \neq 0$,

$$\int dt\, e^{i\omega t} \langle A_k(t) A_k(0) \rangle = 2 \sin^2(kd/2) C(k,\omega), \tag{2.7}$$

with

$$A_k = (N)^{1/2} \sum_{n=1}^{N} e^{-iknd} (x_n - x_{n-1}) , \tag{2.8}$$

where $\langle A_k(t) A_k(0) \rangle$, is the correlation function studied in Refs. 9 and 10.

The frequency moments of $C(k,\omega)$ are defined by

$$\mu_n(k) = \int_{-\infty}^{+\infty} d\omega\, \omega^n\, C(k,\omega) . \tag{2.9}$$

Since, from the definition (2.5), $C(k,\omega)$ is an even function of both k and ω, the odd frequency moments are vanishing. Taking into account the stationary properties of the system, the last ones can be rewritten as[15]

$$\mu_{2n}(k) = \frac{2\pi}{N} \sum_{ij} e^{-ikd(i-j)} \left\{ -2 \langle\, \hat{x}^2 \,\rangle \delta_{n0} + \left[\left\langle \hat{x}_i^{(n)} \hat{x}_j^{(n)} \right\rangle + \left\langle \hat{x}_j^{(n)} \hat{x}_i^{(n)} \right\rangle \right] \right\} . \tag{2.10}$$

where we have used the short notation

$$\hat{x}_i^{(m)} = \frac{d^m}{dt^m}\,\hat{x}_i(t)\bigg|_{t=0} \quad . \tag{2.11}$$

III. THE EFFECTIVE POTENTIAL AND QUANTUM AVERAGES

The time derivatives of the particle position appearing in Eq. (2.10) can be easily obtained from the equations of motion, so that we are only faced with the problem of evaluating equilibrium averages of functions of coordinates and conjugate momenta. This last step is straightforward in the classical case, where it reduces to the calculation of phase space integrals, which can be separated in Gaussian integration over the conjugate momenta and configuration integrals, whose evaluation can be done without particular problems for one-dimensional lattices.[16] In the quantum case, the formula

$$\langle \hat{A} \rangle = \frac{1}{Z}\int d\mathbf{X}\, A(i\hbar\partial_{\mathbf{z}}, \mathbf{X}-\tfrac{1}{2}\mathbf{z})\rho(\mathbf{X}-\tfrac{1}{2}\mathbf{z}, \mathbf{X}+\tfrac{1}{2}\mathbf{z})\bigg|_{\mathbf{z}=0} \tag{3.1}$$

has to be used, where Z is the partition function, $A(p,q)$ the p-q ordered form of A and $\rho(\mathbf{X}', \mathbf{X})$ the (non-normalized) density matrix. An approximate explicit expression for ρ, which finally allows us to reduce the evaluation of equilibrium quantum averages to classical configuration integrals, can be obtained by treating the pure-quantum part of the fluctuations in a self-consistent Gaussian approximation.[17,18,15] In such a way one is able to account for the full quantum behavior of the harmonic excitations of the systems and the full classical nonlinear behavior, the leading nonlinear quantum corrections being also considered. Within such an approach, one obtains

$$\begin{aligned}\rho(\mathbf{X}-\tfrac{1}{2}\mathbf{z}, \mathbf{X}+\tfrac{1}{2}\mathbf{z}) = \left(\frac{m}{2\pi\hbar^2\beta}\right)^{N/2} \int d\mathbf{x}\, e^{-\beta V_G(\mathbf{x})} \\ \times \prod_k \exp\left[\frac{1}{2\hbar^2}\left(\gamma_k(\mathbf{x}) + \frac{m}{\beta}\right) z_k^2\right] \\ \times \prod_k \frac{1}{\left[2\pi\alpha_k(\mathbf{x})\right]^{1/2}} \exp\left[-\frac{1}{2\alpha_k(\mathbf{x})}\left(X_k - x_k\right)^2\right] .\end{aligned} \tag{3.2}$$

Here and in the following the subscript k denotes variables transformed by the orthogonal matrix $U_{ki}(\mathbf{x})$, which diagonalizes the frequency matrix

$$\omega_{ij}^2(\mathbf{x}) = \frac{1}{m}\left\langle \frac{\partial^2 V}{\partial x_i \partial x_j}(\mathbf{x}+\xi)\right\rangle_{\mathbf{x}} \quad , \tag{3.3}$$

whose eigenvalues are $\omega_k(\mathbf{x})$. In Eq. (3.3) we have introduced the notation $\langle f(\xi)\rangle_{\mathbf{x}}$ for the (x-dependent) Gaussian average over the *pure-quantum fluctuation* variables $\boldsymbol{\xi} = \{\xi_i\}$, defined by

$$\left\langle f(\boldsymbol{\xi})\right\rangle_{\mathbf{x}} \equiv \int d\boldsymbol{\xi}\; f(\boldsymbol{\xi}) \prod_k \frac{e^{-\xi_k^2/2\alpha_k(\mathbf{x})}}{\left[2\pi\alpha_k(\mathbf{x})\right]^{1/2}} \quad . \tag{3.4}$$

The parameters

$$\alpha_k(\mathbf{x}) \equiv \frac{\hbar}{2m\omega_k(\mathbf{x})}\left(\coth f_k(\mathbf{x}) - \frac{1}{f_k(\mathbf{x})}\right) \tag{3.5}$$

and

$$\gamma_k(\mathbf{x}) \equiv m^2\omega_k^2(\mathbf{x})\;\alpha_k(\mathbf{x}) \quad , \tag{3.6}$$

with $f_k(\mathbf{x}) = \frac{1}{2}\beta\hbar\omega_k(\mathbf{x})$, are the pure-quantum contribution to the Gaussian fluctuations of position and momentum, respectively, for a harmonic oscillator of frequency $\omega_k(\mathbf{x})$. Finally, the effective potential $V_G(\mathbf{x})$ is given by

$$\begin{aligned}V_G(\mathbf{x}) = \langle V(\mathbf{x}+\xi)\rangle_{\mathbf{x}} - \frac{1}{2}\sum_{ij}\alpha_{ij}(\mathbf{x})\left\langle \frac{\partial^2 V}{\partial x_i \partial x_j}(\mathbf{x}+\boldsymbol{\xi})\right\rangle_{\mathbf{x}} \\ + \frac{1}{\beta}\sum_k \ln\frac{\sinh f_k(\mathbf{x})}{f_k(\mathbf{x})} \quad ,\end{aligned} \tag{3.7}$$

where $\alpha_{ij} = \sum_k U_{ki}U_{kj}\alpha_k$, and the expression for the partition function simplifies to

$$Z = e^{-\beta F} = \left(\frac{m}{2\pi\hbar^2\beta}\right)^{N/2}\int d\mathbf{x}\, e^{-\beta V_G(\mathbf{x})} \quad . \tag{3.8}$$

In order to proceed with the explicit calculations for a many-body system, like the one we are interested in, a further approximation, valid when the nonlinear quantum effects are small, can be introduced.[18,15] Such a low coupling approximation (LCA) relies on the expansion of the frequencies $\omega_k(\mathbf{x})$, and of all the renormalization parameters depending on them, around the configuration $\mathbf{x}_0$ corresponding to the (self-consistent) absolute minimum of $V_G(\mathbf{x})$, in such a way that the implicit dependence on x is removed. Due to the translation symmetry of the system, the configuration $\mathbf{x}_0$ corresponds to uniformly spaced particles with lattice constant d, so that the transformation U_{ki} is reduced to a space Fourier transformation. Within LCA the effective potential for a system with pairwise additive interaction turns out to be again pairwise additive, and for our one-dimensional model we have

$$V_G(\mathrm{x}) = \sum_{i=1}^{N} v_G(x_i - x_{i-1}) \ , \tag{3.9}$$

with

$$v_G(x) = \tilde{v}(x) - \frac{1}{2}\tilde{v}''(d)\mathcal{D} + H \tag{3.10}$$

where

$$\tilde{v}(x) = \left\langle v(x + \xi_i - \xi_{i-1}) \right\rangle_{\mathrm{x}_0} = \sum_{\ell=0}^{\infty} \frac{1}{\ell!} v^{(2\ell)}(x) \left(\frac{\mathcal{D}}{2}\right)^{\ell} \ . \tag{3.11}$$

In the above equations two renormalization parameters have been introduced:

$$H = (N\beta)^{-1} \sum_k (\ln \sinh f_k - \ln f_k) \ , \tag{3.12}$$

which restores the quantum behavior of the harmonic excitations, and

$$\mathcal{D} = N^{-1} \sum_k 4 \sin^2 (kd/2) \ \alpha_k, \tag{3.13}$$

which describes the pure-quantum square fluctuations of the bond length, so it is a renormalization parameter that typically occurs for one-dimensional systems with nearest-neighbor interactions only. Both H and $\mathcal{D}$ in Eq. (3.10) are evaluated using for the frequencies the self-consistent expression:

$$\omega_k^2 = \frac{\tilde{v}''(d)}{m} \ 4 \ \sin^2\left(\frac{kd}{2}\right) \ . \tag{3.14}$$

Once Eq. (3.10) is inserted in Eq. (3.8), the configuration integral can be easily evaluated by applying the methods described in,[19,16] so that, apart from an inessential additive constant, the free energy per particle f results:

$$f = -k_B T \left[\frac{1}{2} \ln\left(\frac{m k_B T}{2\pi\hbar^2}\right) + s_0 d + \ln \mathcal{F}_G(s_0)\right] \ , \tag{3.15}$$

where

$$\mathcal{F}_G(s) = \int_{-\infty}^{\infty} dx \ e^{-sx} \ e^{-\beta v_G(x)} \ , \tag{3.16}$$

and s_0 is fixed by the saddle-point condition for the integral appearing in Eq. (3.8)

$$\frac{1}{\mathcal{F}_G(s)} \left.\frac{d\mathcal{F}_G(s)}{ds}\right|_{s=s_0} = -d \ . \tag{3.17}$$

The actual derivation of explicit expressions for the classical and quantum moments, up to the sixth one, for a general nearest-neighbor interaction potential is described in detail in Ref. 15. Here we report only the final results for the LCA quantum moments:

$$\mu_0(k) = 4\pi \left[\left(\frac{\mathcal{F}_G''(s_0)}{\mathcal{F}_G(s_0)} - d^2\right) \frac{1}{4\sin^2(kd/2)} + \alpha_k + \sigma_k \delta v_2\right] \ , \tag{3.18}$$

$$\mu_2(k) = 4\pi \left[\frac{k_B T}{m} + \omega_k^2 \alpha_k + \omega_k^2 (\alpha_k + \sigma_k) \delta v_2\right] \ , \tag{3.19}$$

$$\mu_4(k) = 4\pi\omega_k^2 \left[\frac{k_B T}{m}\left(\mathcal{W}_{2G} + \frac{\mathcal{D}}{2} v^{iv}(d)\right) \frac{1}{\tilde{v}''(d)} + \omega_k^2 \alpha_k + \omega_k^2 (2\alpha_k + \sigma_k) \delta v_2 + \frac{k_B T}{m} \frac{\mathcal{D}}{2} \delta v_4\right] \ , \tag{3.20}$$

$$\begin{aligned}\mu_6(k) = 4\pi \Bigg\{ & \frac{k_B T}{m^3} \Bigg[\left(\mathcal{W}_{2G}^2 + \tilde{v}''(d) v^{iv}(d) \mathcal{D} - \frac{1}{2} v'''(d)^2 (\mathcal{D} - \overline{\mathcal{D}})\right) \frac{m^2}{\tilde{v}''(d)^2} \ \omega_k^4 \\ & + \left[2\left(\mathcal{W}_{22G} - \mathcal{W}_{2G}^2\right) + v'''(d)^2 (3\mathcal{D} - \overline{\mathcal{D}})\right] \frac{m}{\tilde{v}''(d)} \ \omega_k^2 \Bigg] + \omega_k^6 \alpha_k + \omega_k^6 (3\alpha_k + \sigma_k) \delta v_2 \\ & + \frac{k_B T}{m^2} \ \omega_k^2 \left[\frac{v'''(d)^2}{\tilde{v}''(d)} \ (3\delta\mathcal{D} - \delta\overline{\mathcal{D}}) \ + m\omega_k^2 \left(\frac{v^{iv}(d)}{\tilde{v}''(d)} (\mathcal{D} + \delta\mathcal{D}) - \frac{v'''(d)^2}{2\tilde{v}''(d)^2} (\delta\mathcal{D} - \delta\overline{\mathcal{D}})\right)\right] \delta v_2 \\ & + \frac{2 k_B T}{m^2} \ \omega_k^2 \left[v'''(d) \left(3\mathcal{D} - \overline{\mathcal{D}} - \frac{\mathcal{D} - \overline{\mathcal{D}}}{2} \frac{m\omega_k^2}{\tilde{v}''(d)}\right)\right] \delta v_3 \Bigg\} \ .\end{aligned} \tag{3.21}$$

The new renormalization parameters introduced above are

$$\overline{\mathcal{D}} = \frac{1}{N}\sum_k 4\sin^2\left(\frac{kd}{2}\right)\left[\cos^2\left(\frac{kd}{2}\right)-1\right]\alpha_k \ ,$$
$$\delta\mathcal{D} = \frac{1}{N}\sum_k 4\sin^2\left(\frac{kd}{2}\right)\sigma_k \ ,$$
$$\delta\overline{\mathcal{D}} = \frac{1}{N}\sum_k 4\sin^2\left(\frac{kd}{2}\right)\left[\cos^2\left(\frac{kd}{2}\right)-1\right]\sigma_k \ ,$$
$$\sigma_k = \frac{\omega_k}{2}\frac{\partial\alpha_k}{\partial\omega_k} \ , \tag{3.22}$$

and

$$\delta v_n = \frac{\mathcal{W}_{nG} - v^{(n)}(d)}{\tilde{v}''(d)} \ . \tag{3.23}$$

Finally, the constants $\mathcal{W}_G$ have been defined as follows:

$$\mathcal{W}_{nG} = \frac{1}{\mathcal{F}_G(s_0)}\int_{-\infty}^{\infty} dx\ v^{(n)}(x)\ e^{-s_0x-\beta v_G(x)} \ , \tag{3.24}$$

$$\mathcal{W}_{nmG} = \frac{1}{\mathcal{F}_G(s_0)}\int_{-\infty}^{\infty} dx\ v^{(n)}(x)\ v^{(m)}(x)\ e^{-s_0x-\beta v_G(x)} \ , \tag{3.25}$$

where $v^{(n)}(x)$ denotes the nth derivative of $v(x)$ with respect to its argument.

The classical moments can be easily deduced from the quantum ones by simply dropping all the terms proportional to α_k and σ_k or $\mathcal{D}$ and $\overline{\mathcal{D}}$, and by using the bare potential $v(x)$ instead of v_G or $\tilde{v}(x)$ in Eqs. (3.18)–(3.21) and in the definition of $\mathcal{F}$ and $\mathcal{W}$, which in the classical case will be denoted without the subscript G. For the classical lattice, starting from

$$\frac{d^4x_i}{dt^4} = \frac{1}{m^2}\sum_n \frac{\partial^2 V}{\partial x_i\partial x_n}\frac{\partial V}{\partial x_n} - \frac{1}{m^3}\sum_{n,l}\frac{\partial^3 V}{\partial x_i\partial x_n\partial x_l}p_lp_n, \tag{3.26}$$

we have obtained also the expression for the eighth moment, which at the end comes out to be

$$\mu_8^{(C)}(k) = 4\pi\frac{k_BT}{m^4}\Big[64\sin^6(kd/2)\mathcal{W}_2^3 + 16\sin^4(kd/2)(-4\mathcal{W}_2^3 - 3k_BT\mathcal{W}_3^2 + 4\mathcal{W}_2\mathcal{W}_{22})$$
$$+4\sin^2(kd/2)(2\mathcal{W}_2^3 + 6k_BT\mathcal{W}_3^2 - 6\mathcal{W}_2\mathcal{W}_{22} + 12k_BT\mathcal{W}_{33} + 4\mathcal{W}_{222})\Big]. \tag{3.27}$$

IV. THE MOMENTS OF THE SPECTRAL SHAPE OF THE TODA LATTICE

The application of the above formalism to the Toda lattice is made relatively easy by the form of the interaction potential. In fact, when Eq. (3.10) is considered, it is immediately seen that the effective potential has the same form of the original one:

$$v_G(r) = \frac{a'}{b}\left[e^{-b(r-r_0)}-1\right] + a'(r-r_0) + p'r + C \ , \tag{4.1}$$

if the following renormalized parameters are defined

$$a' = ae^{\mathcal{D}b^2/2}, \tag{4.2}$$

$$p' = a\left(1-e^{\mathcal{D}b^2/2}\right) \ , \tag{4.3}$$

$$C = H + ar_0\left(e^{\mathcal{D}b^2/2}-1\right) - \frac{a}{b}\left(1-e^{\mathcal{D}b^2/2}+\frac{\mathcal{D}b^2}{2}e^{\mathcal{D}b^2/2}e^{-b(d-r_0)}\right) \ . \tag{4.4}$$

We note that $\mathcal{D}b^2/2 \ll 1$ is a consistency test for the validity of the LCA for the Toda lattice.

The special form of the Toda potential allows us to obtain analytic expressions for the functions $\mathcal{F}$ and $\mathcal{W}$ so that all the macroscopic thermodynamic functions and the moments can be computed. If we define the reduced temperature

$$\theta = \frac{k_BT}{a/b} = \frac{b}{a\beta} \tag{4.5}$$

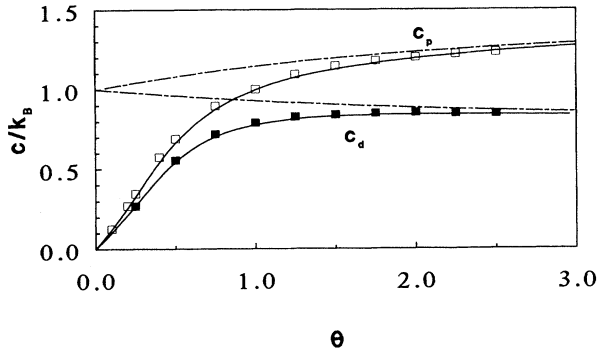

FIG. 1. Specific heat per particle at constant length $d = r_0$ (c_d) and constant pressure $p = 0$ (c_p) of the classical and quantum Toda chain; the quantum results refer to a coupling $g = 1$. Continuous line: Effective potential results; filled and open squares: Bethe-ansatz results (Ref. 21); dot-dashed line: classical result.

and the parameter

$$\eta = e^{\mathcal{D}b^2/2} e^{-b(d-r_0)} \tag{4.6}$$

we have

$$\mathcal{F}(s) = \exp\left[-sr_0 + \eta\frac{\mathcal{D}b^2}{2\theta} + \frac{1}{\theta} - \frac{bH}{a\theta}\right] \times \left(\theta e^{-\mathcal{D}b^2/2}\right)^{(s/b+1/\theta)} \Gamma\left(\frac{s}{b}+\frac{1}{\theta}\right)\frac{1}{b} , \tag{4.7}$$

and s_0 is determined by Eq. (3.17):

$$\ln\left(\theta e^{-\mathcal{D}b^2/2}\right) + \psi\left(\frac{s_0}{b}+\frac{1}{\theta}\right) = b(r_0 - d) , \tag{4.8}$$

where Γ is the Euler gamma function, and ψ its logarithmic derivative. These two equations, together with Eq. (3.15), allow us to obtain all the macroscopic thermodynamic quantities of the system.

The approach based on the effective potential turned out to be valid in many applications. For the thermodynamics of quantum Toda, where exact results are available, a direct comparison has been presented in Ref. 20 where some static correlations were also calculated.

In order to prove the validity of this method, we show in Fig. 1, the temperature behavior of the specific heat at constant lattice length, c_d, for $d = r_0$, and at constant pressure, c_p, for the zero-pressure state, compared with the exact results of the Bethe ansatz.[21] In spite of the rather high coupling $g = 1$, both quantities are in excellent agreement with the exact calculations, and this should allow us to be confident on the moment evaluation.

Turning to the calculation of the quantum moments, we obtain the following results for the functions $\mathcal{W}_G$ of the Toda lattice:

$$\mathcal{W}_{nG} = \frac{a}{b}\,\theta\,(-b)^n e^{-\mathcal{D}b^2/2}\zeta ,$$
$$\mathcal{W}_{nmG} = \left(\frac{a}{b}\right)^2 \theta^2\,(-b)^{n+m} e^{-\mathcal{D}b^2}\zeta(\zeta+1) , \tag{4.9}$$

where $\zeta = (1/\theta + s_0/b)$. Moreover,

$$\delta v_2 = \frac{\delta v_3}{(-b)} = e^{-\mathcal{D}b^2/2}\left(\frac{\theta}{\eta}\zeta - 1\right) \equiv \delta v , \tag{4.10}$$

so that the following expressions for the moments are finally obtained:

$$\mu_0 = \frac{4\pi}{b^2}\,\theta\,\frac{1}{4\eta\sin^2(kd/2)}\left[\frac{\eta}{\theta}\psi'(\zeta) + \overline{\alpha}_k + \overline{\sigma}_k\delta v\right] , \tag{4.11}$$

$$\mu_2 = \frac{4\pi}{b^2}\,\theta\,\omega_0^2\left[1 + \overline{\alpha}_k + (\overline{\alpha}_k + \overline{\sigma}_k)\,\delta v\right] , \tag{4.12}$$

$$\mu_4 = \frac{4\pi}{b^2}\,\theta\,\omega_0^4\,4\eta\sin^2\left(\frac{kd}{2}\right)\left[\frac{\theta}{\eta}\left(1+\frac{\mathcal{D}b^2}{2}\right)e^{-\mathcal{D}b^2/2}\zeta + \overline{\alpha}_k + (2\overline{\alpha}_k + \overline{\sigma}_k)\,\delta v\right] , \tag{4.13}$$

$$\begin{aligned}\mu_6 = \frac{4\pi}{b^2}\,\theta\,\omega_0^6\left[4\eta\sin^2\left(\frac{kd}{2}\right)\right]^2 \Bigg\{ & \left(\frac{\theta}{\eta}\right)^2 e^{-\mathcal{D}b^2}\zeta^2 + e^{-\mathcal{D}b^2/2}\mathcal{D}b^2 - \frac{1}{2}(\mathcal{D}-\overline{\mathcal{D}})b^2 e^{-\mathcal{D}b^2}\left(2\frac{\theta}{\eta}\zeta - 1\right) \\ & + \left[2\left(\frac{\theta}{\eta}\right)^2 e^{-\mathcal{D}b^2}\zeta + (3\mathcal{D}-\overline{\mathcal{D}})b^2 e^{-\mathcal{D}b^2}\left(2\frac{\theta}{\eta}\zeta - 1\right)\right]\frac{1}{4\sin^2(kd/2)} \\ & + \overline{\alpha}_k + (3\overline{\alpha}_k + \overline{\sigma}_k)\,\delta v \\ & + e^{-\mathcal{D}b^2}\left[\frac{(3\delta\mathcal{D}-\delta\overline{\mathcal{D}})b^2}{4\sin^2(kd/2)} + e^{\mathcal{D}b^2/2}(\mathcal{D}+\delta\mathcal{D})b^2 - \frac{(\delta\mathcal{D}-\delta\overline{\mathcal{D}})}{2}b^2\right]\delta v\Bigg\} ,\end{aligned} \tag{4.14}$$

where

$$\overline{\alpha}_k = f_k\coth f_k - 1, \tag{4.15}$$

$$\overline{\sigma}_k = \frac{1}{2}\left(2 - f_k\coth f_k - \frac{f_k^2}{\sinh^2 f_k}\right) . \tag{4.16}$$

Again, the moments of the classical correlation function of the Toda lattice can be deduced from the previous ones by setting to zero all the renormalization constants; the eighth classical moment is given by

$$\mu_8^{(C)} = \frac{4\pi}{b^2}\theta\omega_0^8[4\eta\sin^2(kd/2)]^3\left(\frac{\theta}{\eta}\right)^3\left[\zeta^3 + \frac{\zeta^2}{4\sin^2(kd/2)} + \frac{6\zeta^2+5\zeta}{4\sin^4(kd/a)}\right] . \tag{4.17}$$

V. CONTINUED FRACTION APPROACH TO THE SPECTRAL SHAPE

Starting from the knowledge of the frequency moments, a reconstruction of the correlation function itself can be devised. The naive method consists of expanding the time-dependent correlation function by the series:

$$C(k,t) = \sum_{n=0}^{\infty}(-1)^n\frac{\mu_{2n}}{(2n)!}\,t^{2n} . \tag{5.1}$$

However, this expansion becomes poorly convergent when time increases, and the knowledge of very high-order moments would be necessary to reproduce $C(k,t)$ for long times. A typical behavior is shown in Fig. 2.

A different useful approach can be introduced by considering the following continued fraction representation of the function $C(k,\omega)$:[22–24]

$$C(k,\omega) = \mu_0(k)F(k,\omega) = \mu_0(k)\frac{1}{\pi}\Re e\varphi_0(k,i\omega) \ , \tag{5.2}$$

$$\varphi_0(k,z) \equiv \cfrac{1}{z+\cfrac{\delta_1}{z+\cfrac{\delta_2}{z+\cdots}}} \ , \tag{5.3}$$

where the normalized function $F(k,\omega)$ has been defined. The complex function $\varphi_0(z)$ (the argument k does not play any role in this analysis) can be defined by iterating the recursive equation

$$\varphi_n(z) = \frac{1}{z+\delta_{n+1}\varphi_{n+1}(z)} \ . \tag{5.4}$$

In the time domain, the inverse Laplace transform of $\varphi_n(z)$,$\varphi_n(t)$ is called the nth memory function and obeys, as a consequence of Eq. (5.4), the following generalized Langevin equation

$$\frac{d\varphi_n}{dt} = -\delta_{n+1}\int_0^t d\tau\,\varphi_{n+1}(t-\tau)\varphi_n(\tau) \ . \tag{5.5}$$

The expansion coefficients δ_n are related to the frequency moments.[23,24] The explicit expressions of the first ones are

$$\begin{aligned}
\delta_1 &= \frac{\mu_2}{\mu_0}, \\
\delta_2 &= \frac{\mu_4}{\mu_2} - \frac{\mu_2}{\mu_0}, \\
\delta_3 &= \frac{1}{\delta_2}\left[\frac{\mu_6}{\mu_2} - \left(\frac{\mu_4}{\mu_2}\right)^2\right], \\
\delta_4 &= \frac{1}{\delta_1\delta_2\delta_3}\left(\frac{\mu_8}{\mu_0} - \delta_1^4 - 3\delta_1^3\delta_2 - 3\delta_1^2\delta_2^2 - \delta_1\delta_2^3\right. \\
&\qquad \left. -2\delta_1^2\delta_2\delta_3 - 2\delta_1\delta_2^2\delta_3 - \delta_1\delta_2\delta_3^2\right).
\end{aligned} \tag{5.6}$$

This scheme appears to offer a more manageable expansion for the dynamic response function in terms of static quantities. In the harmonic approximation δ_n vanishes for $n > 1$. For weakly anharmonic systems, the knowledge of the first δ's allows us to reproduce the spectral shape with satisfactory accuracy, by truncating the iteration after some n, i.e., introducing a reasonable approximation of the nth memory function (5.4).[25,26] However, the choice of the termination can be a source of arbitrariness in reconstructing spectral shapes of strongly anharmonic systems, in the absence of some insight into the behavior of the dynamic variables of the system.

In the n-pole approximation,[27] $\delta_n\varphi_n(z)$ is simply approximated by a constant value $1/\tau_n = \delta_n\varphi_n(z{=}0)$, i.e., the more complicated variables associated with the n-th memory function are supposed to have a very short memory (Markov process). The inverse relaxation time

$$\frac{1}{\tau_n} = \delta_n\int_0^\infty dt\,\varphi_n(t) \tag{5.7}$$

is determined assuming a trial functional dependence, e.g., a Gaussian,[27] for $\varphi_n(t)$ or for $\varphi_{n-2}(t)$. In the first case we have $1/\tau_n = \delta_n\sqrt{\pi/2\delta_{n+1}}$, while in the second $1/\tau_n = \sqrt{\pi\delta_{n-1}/2}$, so that the number of δ's to be determined is reduced by two.

In the Gaussian approximation[28,29] at the nth order, the expansion (5.3) is truncated assuming that at a sufficiently high-order n the correlation of the associated dynamical variable[22,23] can be considered a Gaussian with variance δ_{n+1}. The Laplace transform $\varphi_n(z)$ is

$$\varphi_n(z) = \sqrt{\frac{\pi}{2\delta_{n+1}}}\,e^{z^2/2\delta_{n+1}}\left[1-\frac{2}{\sqrt{\pi}}\int_0^{z/\sqrt{2\delta_{n+1}}} e^{-x^2}\,dx\right]. \tag{5.8}$$

We notice that the n pole approximation preserves the first $2n$ moments, all the others being infinite. Instead, the nth-order Gaussian approximation preserves the first $2(n+1)$ moments, while all the others remain finite, determined by the relation

$$\delta_{n+1+m} = (m+1)\delta_{n+1} \ . \tag{5.9}$$

Finally, by calculating the moments of different trial line shapes with two near peaks, we have induced that the existence of such a structure is always connected with

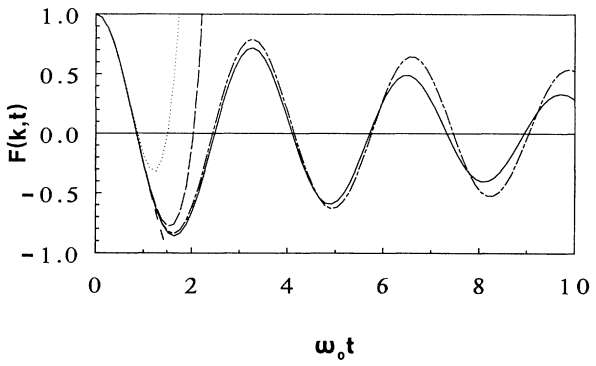

FIG. 2. Normalized classical correlation function $F(k,t) = C(k,t)/\mu_0$ at $\theta = 0.25$ and $kd = \pi$. The Fourier transform of the continued-fraction expansion with Gaussian termination at third order (continuous line) is compared with the numerical solution of the mode-coupling equations (dot-dashed line) and with the series expansion (5.1) truncated at the fourth (dotted line), sixth (dashed line), and eighth (long-dashed line) order.

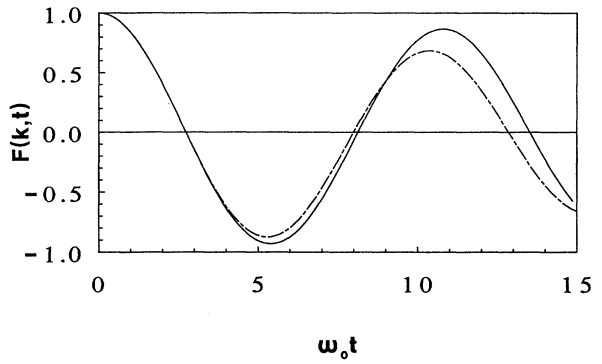

FIG. 3. The same as Fig. 2 at $kd = 0.2\pi$. Only the Fourier transform of the continued-fraction expansion and the mode-coupling results are reported.

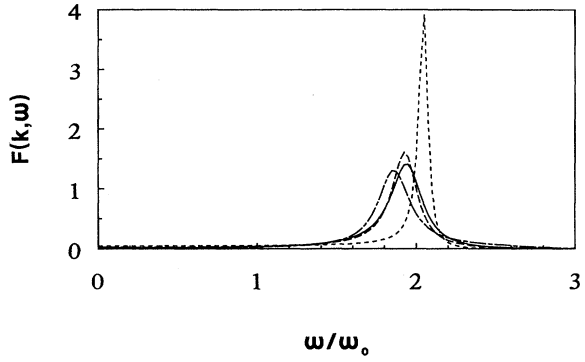

FIG. 4. Comparison between the different termination criteria of the continued-fraction expansion of the normalized classical correlation function. Dashed line: first-order Gaussian; long-dashed line: second-order Gaussian; continuous line: third-order Gaussian; dot-dashed line: five-pole approximation.

the fulfillment of a condition such as

$$\delta_4 \leq \delta_2 << \delta_1 \ . \tag{5.10}$$

VI. RESULTS AND DISCUSSION

Using the aforementioned methods and the equations of the previous sections, we have calculated the classical and quantum moments of $C(k,\omega)$ at different wave vectors and temperatures. Successively, the coefficients of the continued fraction expansions have been evaluated. Some selected results are shown in Tables I–III. All data are reported using reduced units defined in terms of ω_0 and b, and refer to the zero-pressure state.

First, let us notice that the expansion for $C(k,t)$, given in Eq. (5.1), is convergent only for lowest times; adding new terms is less and less significant. This can be seen in Fig. 2, where the classical $C(k,t)$, derived by Fourier transforming the $C(k,\omega)$ obtained by a third-order Gaussian approximation, is displayed for comparison. In Fig. 2 we also report the result of our mode-coupling calculation, done by integrating the equation of motion given in Ref. 9. In the numerical integration a uniform mesh of 160 wave vectors in the Brillouin zone has been considered; the time step used is $\pi/(200\omega_0)$, and the integration has been performed up to $\omega_0 t \simeq 70$. The mode-coupling approach preserves the moments up to the sixth. It turns out to be in agreement with the continued fraction expansion at high k, while it exhibits some differences at low wave vectors (Fig. 3). However, it is important to stress that the mode-coupling is an approximate approach, so that it cannot be considered as a reference test, like a simulation. Although such theories seem to be useful in the study of dynamic critical phenomena[13] as well as in the interpretation of many experimental outcomes,[30,31] no rigorous justification of the underlying approximations is available. Moreover, it is not easy to single out the nature and to estimate the size of the errors introduced by the approximations employed.

Let us make some speculations based on the overall behavior of the coefficients δ_n. We remember that their values are calculated exactly in the classical case. Note that (i) the quantum values tend to approach the classical ones at higher temperatures, as required; (ii) the values of δ_2 are much smaller than δ_1 at least at lower temperatures, signaling the presence of a peak that is narrower for the quantum system; and (iii) the values of δ_4, available for the classical model, are much larger than those of δ_2: they turn out to be of the same order as the classical δ_3, which is independent of k, according to Eqs. (3.18)–(3.21) and (5.6).

This leads to the conclusion that the spectral shapes at low temperatures have to present a single peak close to

TABLE I. Values of the moments and of the coefficients δ_n at the zone boundary in the classical chain and for two different values of the quantum coupling at three selected temperatures.

$kd = \pi$		$\mu_0 b^2$	$\mu_2 b^2/\omega_0^2$	$\mu_4 b^2/\omega_0^4$	$\mu_6 b^2/\omega_0^6$	$\mu_8 b^2/\omega_0^8$	δ_1/ω_0^2	δ_2/ω_0^2	δ_3/ω_0^2	δ_4/ω_0^2
θ=0.1	Clas.	0.331	1.257	5.024	21.092	95.376	3.802	0.196	4.069	2.928
	g=0.4	1.275	5.021	19.985	80.401		3.939	0.0409	4.181	
	g=1	3.172	12.493	49.237	195.394		3.939	0.0021	50.083	
θ=0.25	Clas.	0.892	3.142	12.561	56.502	304.385	3.522	0.477	4.194	4.303
	g=0.4	1.470	5.446	21.603	90.771		3.705	0.262	3.549	
	g=1	3.265	12.441	48.358	190.728		3.811	0.0761	2.914	
θ=1.0	Clas.	5.170	12.566	50.250	301.440	3215.097	2.431	1.568	5.100	10.898
	g=0.4	5.334	13.227	52.392	303.129		2.480	1.481	4.880	
	g=1	6.152	16.411	62.413	309.842		2.668	1.136	3.889	

TABLE II. Values of μ_0 and of the coefficients δ_n at half zone boundary in the classical and quantum chain for two different values of the coupling and at three selected temperatures.

$kd = 0.5\pi$		$\mu_0 b^2$	δ_1/ω_0^2	δ_2/ω_0^2	δ_3/ω_0^2	δ_4/ω_0^2
θ=0.1	Clas.	0.661	1.901	0.0982	4.069	5.926
	g=0.4	1.823	1.960	0.0304	10.148	
	g=1	4.493	1.966	0.0027	80.902	
θ=0.25	Clas.	1.783	1.761	0.238	4.194	7.302
	g=0.4	2.403	1.821	0.167	5.119	
	g=1	4.702	1.883	0.0613	9.199	
θ=1.0	Clas.	10.335	1.215	0.784	5.100	13.897
	g=0.4	10.502	1.228	0.762	5.027	
	g=1	11.350	1.281	0.659	4.690	

$\omega = \sqrt{\delta_1}$. In view of the condition (5.10), doubly peaked structures seem to be inconsistent with the set of calculated δ's, especially at lower wave vectors, where δ_3 and δ_4 are much greater not only than δ_2, but also than δ_1; indeed, their large values would not affect the neighborhood of the single peak strongly enough to transform it into a double peak.

The situation must be similar for the quantum model, even though δ_4 is not available; the much higher values of δ_3 at lowest temperatures indeed make practically ineffective any possible modification of δ_4. The absence of two-peaked structures at any wave vector has been confirmed by recent molecular-dynamics simulations[8] that did not find the "soliton peak." In addition, our mode-coupling calculations also do not exhibit doubly peaked spectral shapes, in contrast with the previous analogous results[9,10] at intermediate wave vectors.

In order to verify the convergence of the continued fraction expansion, we have compared different terminations at increasing stages. One example of this check is displayed in Fig. 4 for the classical case, where more moments, exactly calculated, are available. The Gaussian termination appears to be convergent starting from the second-order one, in agreement with the behavior of δ_4 with respect to δ_3. The n-pole approximation is convergent from the fourth stage and gives similar spectral shapes. This qualifies us to use the second-order Gaussian termination, both for the classical and quantum model, as we do in the following.

The calculated spectral shapes are reported in Figs. 5 and 6, at selected wave vectors, for two different temperatures. As expected, the spectra present a single peak whose position shifts towards lower frequencies as the temperature is raised, and whose width increases with wave vector and temperature. As discussed before, the peak turns out to be centered near the value of $\sqrt{\delta_1}$. Taking into account Eqs. (3.18) and (3.19), this peak shows, at lowest temperature, the k dependence of the phonon excitations. The quantum peaks lie at a frequency slightly higher than the corresponding classical ones, and are narrower. This can be explained by remembering that our approach reduces to the self-consistent quasiharmonic approximation at lowest temperature. Therefore, no damping is present in the quantum system for vanishing temperature. At $T = 0$ and $p = 0$ both the classical and quantum spectra are simply given by δ functions centered at the same frequency. As the temperature increases the frequency shift of the classical peak is more rapid, due to the stronger frequency renormalization of the elementary excitations and the more relevant role of the thermal fluctuations in the classical system is also the reason of the larger damping effects.

VII. CONCLUSION

We have approached the dynamic correlations of the Toda lattice by calculating the first frequency moments of the spectral shape of the displacement-displacement correlation function.

For the classical system, the moments have been exactly calculated up to the eighth one, by an analytic ex-

TABLE III. The same as in Table II, but for the wave vector $kd = 0.2\pi$.

$kd = 0.2\pi$		$\mu_0 b^2$	δ_1/ω_0^2	δ_2/ω_0^2	δ_3/ω_0^2	δ_4/ω_0^2
θ=0.1	Clas.	3.460	0.363	0.0188	4.069	8.352
	g=0.4	4.987	0.368	0.0118	14.273	
	g=1	10.401	0.373	0.0019	77.643	
θ=0.25	Clas.	9.338	0.336	0.0455	4.194	9.728
	g=0.4	9.997	0.339	0.0417	6.285	
	g=1	13.161	0.347	0.0255	12.710	
θ=1.0	Clas.	54.117	0.232	0.150	5.100	16.324
	g=0.4	54.284	0.233	0.149	5.142	
	g=1	55.158	0.235	0.144	5.296	

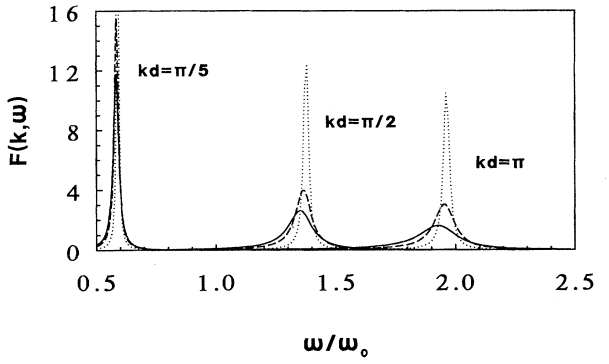

FIG. 5. Normalized classical and quantum correlation function at three selected wave vectors and at $\theta = 0.25$. Continuous line: classical result; dashed line: quantum result with coupling $g = 0.4$; dotted line: quantum result with coupling $g = 1$. The maximum value of $F(k,\omega)$ at $kd = \pi/5$, which lies out of the figure, is 35.78.

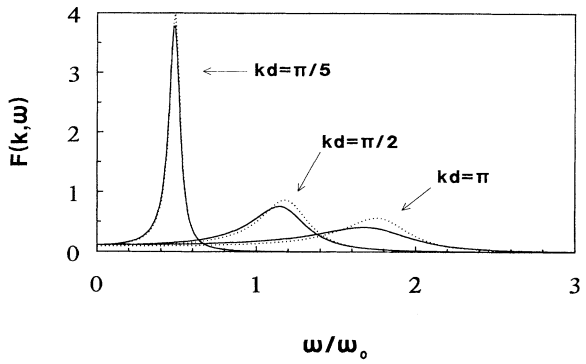

FIG. 6. The same as in Fig. 5 at $\theta = 1.0$. Only the quantum result for coupling $g = 1$ is reported.

pression based on the transfer matrix.[19,16] The analysis of the coefficients of the continued fraction expansion leads to the conclusion that doubly peaked structures are not consistent with the calculated values. The presence of a single peak is confirmed by our mode-coupling calculation, in agreement with recent numerical simulations.[8] Indeed, we have found single-peaked spectral shapes at any wave vectors using both n-pole and Gaussian terminations; we have verified that the second-order Gaussian termination is very near the third one and does not differ much from the four- and the five-pole approximations.

For the quantum system, the moments have been calculated up to the sixth one. We have evaluated the quantum averages by means of the effective potential in low coupling approximation. The range of validity of this calculation at constant pressure, $p = 0$, has been derived by the comparison with exact Bethe-ansatz data for the specific heat for coupling $g = 1$. The very good agreement leads us to be confident of the applicability of the methods at all temperatures for $g \leq 1$. The spectral shapes, calculated by the second-order Gaussian approximation, show a behavior similar to the classical ones, with a narrower single peak. Both in the classical and quantum Toda lattice, the peaks of the spectral shapes can be ascribed to the phonon excitations.

ACKNOWLEDGMENTS

We thank F. Mertens and A. Neuper for information about their simulation data. Useful discussions with A. R. Bishop are also acknowledged. This work was done with the support of the NATO S.P. Chaos, Order and Patterns, (CRG 901098).

[1] S.E. Trullinger *et al.*, *Solitons* (North-Holland, Amsterdam, 1986).
[2] M. Toda, J. Phys. Soc. Jpn. **22**, 431 (1967).
[3] M. Toda, J. Phys. Soc. Jpn. **23**, 501 (1967).
[4] M. Toda, *Theory of Nonlinear Lattices* (Springer, Berlin, 1981).
[5] M. Toda and N. Saitoh, J. Phys. Soc. Jpn. **52**, 3703 (1983).
[6] V.E. Korepin, A.G. Izergin, and N.M. Bogoliubov, *Quantum Inverse Scattering Method, Correlation Functions and Algebraic Bethe Ansatz* (Cambridge University Press, Cambridge, UK, 1992).
[7] T. Schneider and E. Stoll, Phys. Rev. Lett. **45**, 997 (1980).
[8] F.G. Mertens and A. Neuper (private communication).
[9] S. Diederich, Phys. Rev. B **24**, 3186 (1980); **24**, 3193 (1980).
[10] S. Diederich, Phys. Lett. **85A**, 233 (1981).
[11] S. Diederich, Phys. Lett. **86A**, 294 (1981).
[12] M. Blume and J. Hubbard, Phys. Rev. B **1**, 3815 (1970).
[13] K. Kawasaki, in *Phase Transition and Critical Phenomena, Vol. 5a*, edited by C. Domb and M.S. Green (Academic, London, 1976).
[14] F.G. Mertens and H. Büttner, J. Phys. A **15**, 1831 (1982).
[15] A. Cuccoli, V. Tognetti, A.A. Maradudin, A.R. Mc Gurn, and R. Vaia, Phys. Rev. B **46**, 8839 (1992).
[16] A. Cuccoli, V. Tognetti, and R. Vaia, Phys. Lett. A **160**, 184 (1991).
[17] R. Giachetti and V. Tognetti, Phys. Rev. Lett. **55**, 912 (1985).
[18] R. Giachetti and V. Tognetti, Phys. Rev. B **33**, 7647 (1986).
[19] F. Gürsey, Proc. Cambridge Philos. Soc. **46**, 182 (1950).
[20] A. Cuccoli, M. Spicci, V. Tognetti, and R. Vaia, Phys. Rev. B **45**, 10 127 (1992).
[21] M. Hader and F.G. Mertens, J. Phys. A **19**, 1913 (1986).
[22] H. Mori, Prog. Theor. Phys. **33**, 423 (1965).
[23] H. Mori, Prog. Theor. Phys. **34**, 399 (1965).
[24] M. Dupuis, Prog. Theor. Phys. **37**, 502 (1967).
[25] U. Balucani and V. Tognetti, Phys. Rev. B **16**, 271 (1977).
[26] B.J. Berne and R. Pecora, *Dynamic Light Scattering* (Wiley, London, 1976).
[27] S.W. Lovesey and R.A. Meserve, J. Phys. C **6**, 79 (1972).
[28] K. Tomita and H. Tomita, Prog. Theor. Phys. **45**, 1407 (1971).
[29] H. Tomita and H. Mashiyama, Prog. Theor. Phys. **48**, 1133 (1972).
[30] A. Cuccoli, S.W. Lovesey, and V. Tognetti, Phys. Rev. B **39**, 2619 (1989).
[31] A. Cuccoli, S.W. Lovesey, and V. Tognetti, J. Phys. Condens. Matter **2**, 3339 (1990).